Damage localization in offshore structures using shaped inputs

Ulriksen, Martin Dalgaard; Bernal, Dionisio; Nielsen, Morten Eggert; Damkilde, Lars

Published in:
Procedia Engineering

DOI (link to publication from Publisher):
10.1016/j.proeng.2017.09.273

Publication date:
2017

Document Version
Accepted author manuscript, peer reviewed version

Available online at www.sciencedirect.com

SciVerse ScienceDirect

Procedia Engineering 00 (2017) 000–000

Procedia Engineering

www.elsevier.com/locate/procedia

X International Conference on Structural Dynamics, EURODYN 2017

Damage localization in offshore structures using shaped inputs

Martin D. Ulriksen[a,*], Dionisio Bernal[b], Morten E. Nielsen[a], Lars Damkilde[a]

[a]*Department of Civil Engineering, Aalborg University, 6700 Esbjerg, Denmark*
[b]*Civil and Environmental Engineering, Center for Digital Signal Processing, Northeastern University, Boston MAS 02115*

Abstract

Input shaping is an active control procedure by which vibrations in a structural subdomain are suppressed. Recently, a scheme based on shaped inputs has been proposed for damage localization purposes; cast on the premise that the vibration signature of a structural domain in a damaged phase will be identical to the signature of the healthy, reference counterpart if, for the same loading conditions, the subdomain containing damage is inactive in terms of vibrations. The methodological idea is, thus, to apply controllable inputs that are shaped such that particular vibration quantities (depending on the type of damage one seeks to localize) are suppressed in one subdomain at the time, hereby resulting in damage being localized when the vibration signature induced by the shaped inputs in the damaged phase corresponds to that obtained in the reference phase. The present paper treats an application study that illustrates the damage localization scheme in simulations on a finite element (FE) model of an offshore jacket structure exposed to stochastic plane wave fields generated from a directional wave spectrum, and with fluid-structure interaction considered in terms of the Morison equation. In both structural phases, that is, the reference and the damaged one with a single mass perturbation, four inputs to be shaped are applied, and the resulting displacements are extracted from a single spatial location within the model. It is contended that the damage can be localized when suppressing displacements near or, ideally, directly at its location.

Peer-review under responsibility of the organizing committee of EURODYN 2017.

Keywords: Damage localization; Structural health monitoring; Input shaping; Fluid-structure interaction; Offshore structures

1. Introduction

In adherence to the conventional classification, one defines damage characterization as a triad composed of damage detection, localization, and quantification. The present study treats the central piece of this triad—namely, the localization component—in a vibration-based context. Traditionally, vibration-based damage localization methods are cast with the aim of finding damage-induced differences between vibration signatures from the structure in its healthy/reference phase and its damaged one. These damage-induced differences are then mapped to the structural domain; either directly or by use of a theoretical model to enhance the spatial localization resolution. The direct approaches are denoted data-driven and examples can be found in [1], while the approaches implementing a theoretical

* Corresponding author. Tel.: +45-52300716.
E-mail address: mdu@civil.aau.dk

1877-7058
Peer-review under responsibility of the organizing committee of EURODYN 2017.

model, of which examples include the damage location vector (DLV) schemes proposed by Bernal [2–5], are referred to as model-based [6].

Recently, an alternative to these two general approaches has been proposed by Ulriksen et al. [7]. Here, damage is localized in a structural domain by shaping controllable inputs such that certain vibration quantities (depending on the type of damage one seeks to localize) are suppressed in one subdomain at the time. When these vibration quantities are suppressed in the subdomain containing the damage, the response is identical to that which would take place in the absence of the change, provided that the input is the same. As such, one can, in theory, measure any coordinate within the domain and determine if there is a change in the response compared to the signature stored for the reference condition.

The applicability of the input shaping-based damage localization approach has been tested, successfully, in the context of a numerical study with a simple two-dimensional truss structure [7]. The present paper serves to investigate the applicability of the approach for a more complex system, namely, a beam finite element (FE) model of an offshore jacket structure, which, in its damaged phase, is introduced to a single mass perturbation. The model is, in both structural phases, subjected to ambient excitation—in the form of stochastic plane wave fields generated from a directional wave spectrum—and four controllable, harmonic inputs. It is, thus, contended that the mass perturbation can be localized by interrogating one structural subdomain at the time by shaping the harmonic inputs accordingly.

The paper is organized as follows. In section 2, a brief review of the procedure of shaping harmonic inputs is provided, and subsequently, in section 3, the premise of applying shaped inputs to localize mass perturbations is outlined. Section 4 presents the numerical example with the offshore jacket structure and, lastly, some concluding remarks are given in section 5.

2. Shaping harmonic inputs

Consider an undamaged structural domain that is discretized with n degrees of freedom (DOF) and subjected to p controllable, harmonic inputs, which act in the DOF indexed by $\mathcal{T} = \{\mathcal{T}_1, \mathcal{T}_2, \dots, \mathcal{T}_p\} \subset \mathcal{S}$, with $\mathcal{S} = \{1, 2, \dots, n\}$. Under the assumptions of linearity and time-invariance, the temporal equilibrium equation becomes

$$M\ddot{x}(t) + C\dot{x}(t) + Kx(t) = f(t), \tag{1}$$

where K, C, $M \in \mathbb{R}^{n\times n}$ are the stiffness, damping, and mass matrices, x_u, $\dot{x}_u$, $\ddot{x}_u \in \mathbb{R}^n$ are the nodal displacement, velocity, and acceleration vectors, and $f \in \mathbb{R}^n$ is the nodal load vector.

The basic idea of input shaping is to shape the p inputs such that particular kinematic quantities, resulting solely from these inputs, are suppressed in a subdomain of the structure in question [8]. In the following, it is, for the sake of simplicity and without loss of generality, assumed that only the shaped inputs affect the structure, thus

$$\forall j \in \mathcal{T} : f_j(t) = a_j \cos\left(\omega t + \theta_j\right), \qquad \forall j \in \mathcal{S} \setminus \{\mathcal{T}\} : f_j(t) = 0. \tag{2}$$

For such harmonic inputs, the steady-state output can be expressed in frequency domain as

$$x(\omega) = (-M\omega^2 + Ci\omega + K)^{-1} f(\omega) = G(\omega) f(\omega) = G_{\mathcal{T}}(\omega) f_{\mathcal{T}}(\omega), \tag{3}$$

with $G_{\mathcal{T}}$ being the frequency response matrix columns corresponding to the input DOF, while $x(\omega) = \mathcal{F}(x(t))$ and $f(\omega) = \mathcal{F}(f(t))$ are the Fourier transforms of the output and the input, respectively. The task, therefore, becomes that of shaping $a_{\mathcal{T}}$ and $\theta_{\mathcal{T}}$ such some linear transformation

$$T : x \in \mathbb{C}^n \mapsto u \in \mathbb{C}^q \tag{4}$$

is suppressed; that is,

$$u = TG_{\mathcal{T}} f_{\mathcal{T}} = 0 \tag{5}$$

in which explicit reference to the frequency variable is omitted for convenience. We note that $TG_{\mathcal{T}} \in \mathbb{C}^{q\times p}$, and provided that $p > q$, this matrix has a null space, $\mathrm{Null}\,(TG_{\mathcal{T}}) \in \mathbb{C}^{p\times(p-q)}$, from where relative values of $a_{\mathcal{T}}$ and $\theta_{\mathcal{T}}$ that yield $u = 0$ can be selected.

3. Localizing mass perturbations by shaped inputs

3.1. Suppressing mass perturbations

Let damage be manifested as a mass perturbation, ΔM, that acts physically in the DOF subset indexed by $\mathcal{V} \subset \mathcal{S}$. Then, the temporal equilibrium equation for the same loading conditions as in eq. (1) becomes

$$M\ddot{\tilde{x}}(t) + C\dot{\tilde{x}}(t) + K\tilde{x}(t) = f(t) + \Delta M\ddot{\tilde{x}}(t), \tag{6}$$

where $\sim$ refers to damaged conditions. Introducing $\Delta x = \tilde{x} - x$ and subtracting eq. (1) from eq. (6), one obtains

$$M\Delta\ddot{x}(t) + C\Delta\dot{x}(t) + K\Delta x(t) = \Delta M\ddot{\tilde{x}}(t), \tag{7}$$

from which it is evident that direct suppression of $u = \tilde{x}_{\mathcal{V}}$ will yield $\Delta M\ddot{\tilde{x}}(t) = 0$ and, as such, $\tilde{x} = x$. Thus, when the DOF in which the mass perturbation acts are inactive, the response in the damaged phase is identical to that which would take place in the absence of the damage. From eq. (5), it is clear that the number of inputs to apply is governed by the rank of the introduced damage, as $q = \operatorname{rank}(\Delta M)$ such $p > \operatorname{rank}(\Delta M)$ to provide a null space of $TG_{\mathcal{T}}$ from which the inputs can be extracted.

3.2. Structural interrogation and signature discrimination

When interrogating a structural domain for the location of a mass perturbation, the linear mapping in eq. (5) yields $u(\omega) = x_{\mathcal{U}^{(z)}}(\omega)$, where $x_{\mathcal{U}^{(z)}}$ is a particular DOF subset with q or fewer elements. The procedure is, as such, to suppress a DOF subset one z at the time. Under realistic conditions, where ambient vibrations and other disturbances are present, we note that $\Delta x \neq 0$; even if $\mathcal{U}^{(z)} \supseteq \mathcal{V}$. In these cases, the added harmonic inputs must be shaped such that they suppress the steady-state output induced by themselves, hence

$$x_{\mathcal{U}^{(z)}}(\omega) = w_{\mathcal{U}^{(z)}}(\omega) \tag{8}$$

where $w_{\mathcal{U}^{(z)}}(\omega)$ contains the ambient vibrations in DOF number $\mathcal{U}^{(z)}$ for the reference phase. It follows that if $\mathcal{U}^{(z)} \supseteq \mathcal{V}$, one gets

$$\tilde{x}_{\mathcal{U}^{(z)}}(\omega) = \tilde{w}_{\mathcal{U}^{(z)}}(\omega), \tag{9}$$

while

$$\forall \mathcal{U}^{(z)} \not\supseteq \mathcal{V} : \; \tilde{x}_{\mathcal{U}^{(z)}}(\omega) = \tilde{x}_{I,\mathcal{U}^{(z)}}(\omega) + \tilde{w}_{\mathcal{U}^{(z)}}(\omega), \tag{10}$$

with $\tilde{w}_{\mathcal{U}^{(z)}}(\omega)$ and $\tilde{x}_{I,\mathcal{U}^{(z)}}(\omega)$ being the ambient and steady-state (from the shaped inputs) displacements in the damaged phase.

In the present study, we measure the output in a single DOF, indexed by $\mathcal{Y}$. In this context, the task becomes that of evaluating whether $\tilde{x}^{(z)}_{\mathcal{Y}}(\omega)$ deviates significantly from the underlying distribution of $x^{(z)}_{\mathcal{Y}}(\omega)$. The approach suggested in [7] is to establish a statistical baseline model based on a number of experiments in the healthy phase and then testing the discordance between $\tilde{x}^{(z)}_{\mathcal{Y}}$ and this baseline model. In the present study, however, the discordance measure is simply taken as the root-mean-square error (RMSE)

$$R^{(z)} = \sqrt{\frac{\sum_{i=1}^{N}\left(|\tilde{x}^{(z)}_{\mathcal{Y},i}| - |x^{(z)}_{\mathcal{Y},i}|\right)^2}{N}}, \tag{11}$$

where N is the number of samples in each measurement sequence.

4. Numerical example

The input shaping-based damage localization approach is tested in the context of simulations on a numerical model of a bottom-founded offshore jacket structure, which is exposed to ambient excitation and four controllable, harmonic inputs. It is noted that, for simplicity, a transition piece and a superstructure (often composed of a wind turbine) are omitted.

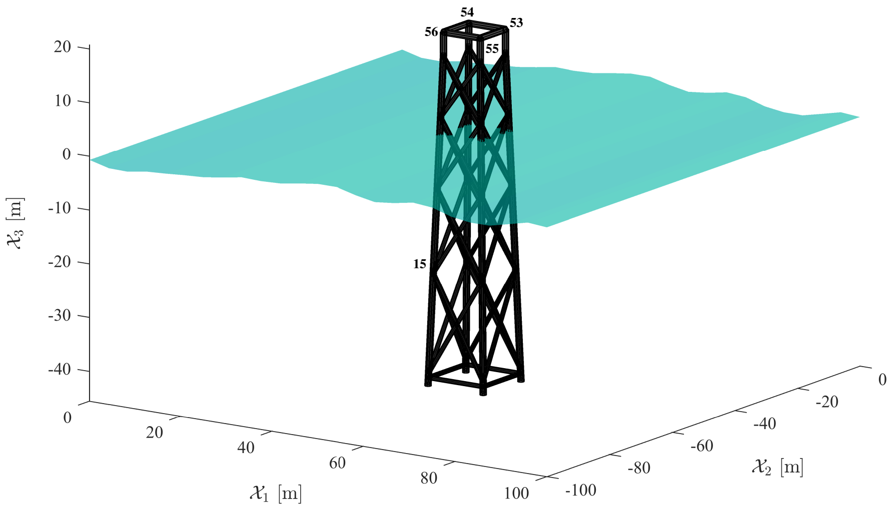

Fig. 1: FE model of bottom-founded jacket structure exposed to harmonic inputs (acting in $\mathcal{X}_1$-direction) in nodes 53–56 and plane wave fields. The $\mathcal{X}_1$-directional displacement response is captured in node 56. In the damaged phase, a mass perturbation is added in node 15.

4.1. Fluid-structure modeling

The jacket structure, which is depicted in fig. 1, is modeled as an approximately 66 m high space frame by use of 108 Timoshenko beam elements, yielding 336 DOF of which 24 are fixed to the seabed. Therefore, we will operate with a reduced DOF set indexed by $\mathcal{S} = \{1, 2, \ldots, 312\}$. The model is assigned a Rayleigh damping distribution with the damping ratio of the first bending mode in $\mathcal{X}_1$-direction being 0.05. Four harmonic inputs to be shaped are applied at nodes 53–56 with the driving frequency $\omega = (\omega_1 + \omega_2)/2$, where ω_i is the eigenfrequency of the i'th bending mode in $\mathcal{X}_1$-direction. In addition, since the structure is assumed situated at an offshore location with a water depth of approximately 46 m, it is exposed to ambient wave excitation. This excitation is modeled as stochastic plane wave fields with a significant wave height of 1 m and a peak period of 8 s, which are generated from a JONSWAP wave spectrum [9] and coupled to the structural domain by use of the Morison equation [10]. All analyses are conducted in the numerical simulation tool SOFIA, developed by Nielsen et al. [11] who provide a more detailed description of the fluid-structure modeling implemented in the present example.

The structure is analyzed in two phases, namely, a healthy one and a damaged one with a mass perturbation in node 15. The perturbation corresponds to 1 % of the entire mass of the healthy structure, and it is contended that this perturbation can be localized by comparison of the shaped output across the structural phases. The output is taken, with a sampling frequency of 500 Hz, as $\mathcal{X}_1$-directional displacements in node 56, which are contaminated with 5 % white Gaussian noise.

4.2. Input shaping

The mass perturbation is introduced such that it acts in all translational DOF in node 15 (corresponding to DOF number 67–69), thus the requirement of $p > \text{rank}(\Delta M) = 3$ is complied with, since $p = 4$ inputs are utilized. In fig. 2, the normalized amplitudes of the steady-state responses induced solely by the harmonic inputs are plotted for the free DOF when shaping to suppress the translational DOF in node 15. As evidenced, the amplitudes are, for all practical purposes, zero in DOF number 67, 68, and 69, hereby validating the procedure documented in section 2

In the case where both the shaped inputs and the wave loading are applied to the structure, the response will generally be a superposition of the response due to each of the two loading components. Yet, in the DOF for which the harmonic inputs are shaped, the response will only contain wave load contributions when steady-state conditions are obtained for the response induced by the shaped inputs. This is illustrated in fig. 3 for the case where the harmonic inputs are shaped to suppress DOF number 67–69 in the healthy structure. Fig. 3a shows the total response in

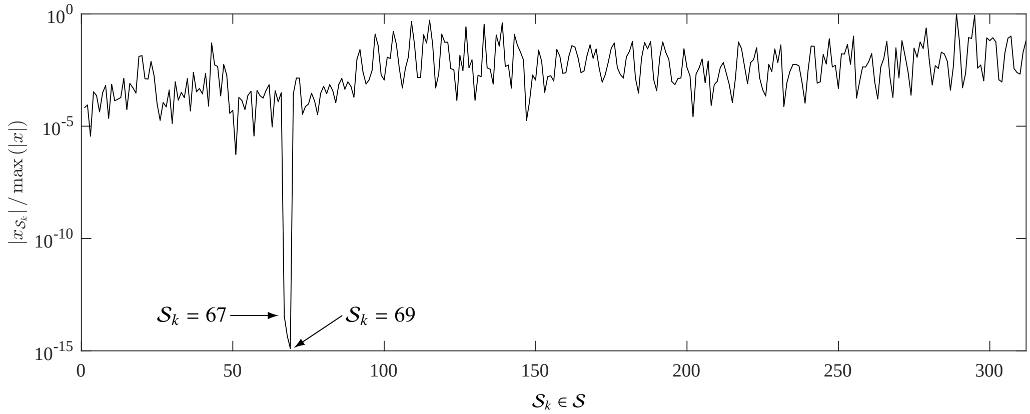

Fig. 2: Suppression of translational DOF in node 15, corresponding to DOF number 67–69. Eq. 5 is directly employed without simulations.

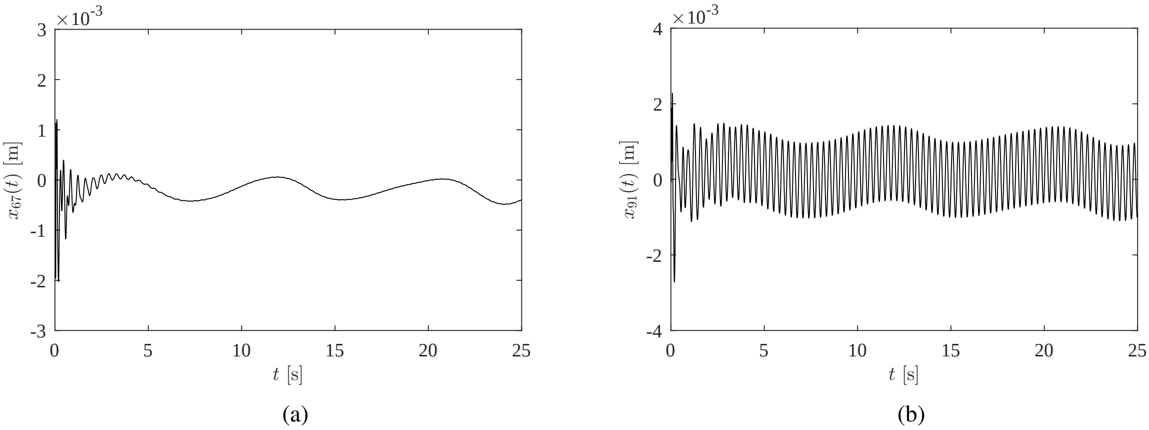

Fig. 3: Noise-free displacement responses in the jacket structure excited by shaped inputs and a plane wave field. (a) $x_{67}(t)$. (b) $x_{91}(t)$.

DOF number 67 while fig. 3b shows the total response in DOF number 91, which is the $\mathcal{X}_1$-directional displacement component in node 20 (the "corresponding" node in an adjacent jacket leg).

4.3. Structural interrogation

It is contended that when the steady-state displacements in DOF number 67–69 are suppressed, the signature from the damaged structural phase will differ from that of the reference one only by means of the ambient vibrations, whereas the signature deviations if suppressing the steady-state displacements in any other DOF triad combination will include vibrations governed by the shaped inputs. This is tested by shaping the inputs to suppress the steady-state response in one DOF subset at the time in the undamaged phase and then comparing this vibration signature, through eq. (11), with the one obtained by applying these inputs (plus ambient excitation) to the damaged structure.

In the interrogations, it is chosen only to focus on the translational DOF, and since it is assumed that nodes 1–4 are fixed and that nodes 53–56 do not contain damage, a total of 48 interrogation patterns exist. In figure fig. 4, the interrogation results, taken as RMSEs from eq. (11), are shown. Evidently, the smallest RMSE is obtained when interrogating DOF number 67, 68, and 69, which, as stated previously, are the ones affected by damage. Thus, the damage is localized, but the resolution is—despite taking the added mass as 1 % of the jacket mass—not impressive, as the second smallest RMSE, $R^{(11)}$, is only two times larger than $R^{(12)}$. However, in this context, it is worth noting that $z = 11$ comprises the combination for the node below node 15 (containing damage), hereby implying that the approach also has merit in cases where only spatial locations close to, but not at, the structural subdomain containing damage are interrogated. Additionally, it has been observed that distributing more sensors, in particular, some under

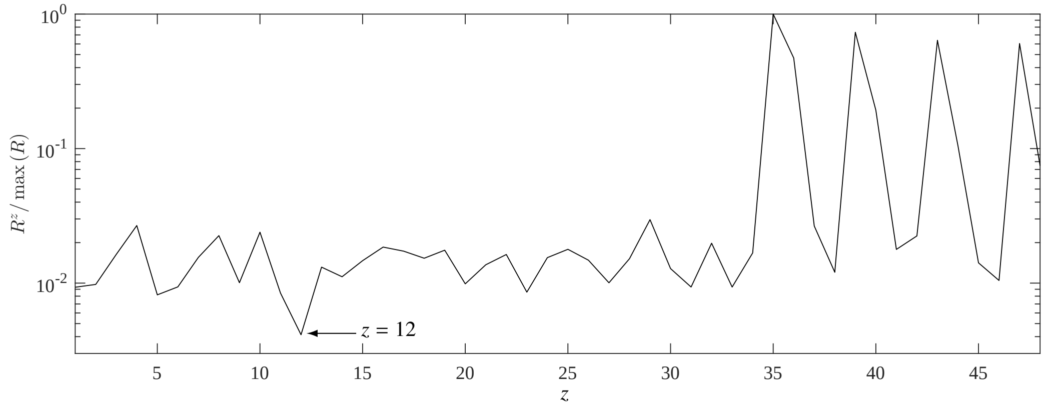

Fig. 4: Normalized RMSEs from interrogation of 48 DOF combinations, with damage being manifested in DOF combination $z = 12$.

the sea level, to capture the response generally enhances the resolution, and it is also contended that the resolution can be further improved by implementing a more sophisticated statistical discrimination technique, see, for example, [7].

5. Conclusion

The input shaping-based damage localization scheme constitutes a conceptual alternative to the traditional vibration-based damage localization methods, which, typically, operate on the premise of mapping damage-induced vibration signature deviations to the structural domain. Instead, the input shaping approach localizes structural damage by applying a controllable load distribution for which the steady-state response of the structure is the same in the two structural phases.

The applicability of the input shaping-based approach has been tested in the context of a numerical model of an offshore jacket structure exposed to plane wave fields. Four controllable, harmonic inputs have been applied to interrogate the structural domain with respect to a mass perturbation of 1 % of the entire structural mass, acting in all translational DOF in a single node below the sea level. It is found that the approach facilitates localization, albeit with a rather poor resolution that, however, has been found to improve as multiple sensors are used in the interrogations. Obviously, numerous studies addressing, for example, how to enhance the resolution must be conducted before a general conclusion can be drawn on the applicability, but the feature of allowing for localization of damage under the sea level strictly by use of equipment (to provide the input and measure the output) above sea level seems auspicious.

References

[1] W. Fan, P. Qiao, Vibration-based damage identification methods: A review and comparative study, Structural Health Monitoring 10 (2011) 83–111.
[2] D. Bernal, Load vectors for damage localization, Journal of Engineering Mechanics 128 (2002) 7–14.
[3] D. Bernal, Flexibility-based damage localization from stochastic realization results, Journal of Engineering Mechanics 132 (2006) 651–658.
[4] D. Bernal, Damage localization from the null space of changes in the transfer matrix, AIAA Journal 45 (2007) 374–381.
[5] D. Bernal, Load vectors for damage location in systems identified from operational loads, Journal of Engineering Mechanics 136 (2010) 31–39.
[6] C. R. Farrar, K. Worden, Structural Health Monitoring: A Machine Learning Perspective, 1 ed., John Wiley & Sons, 2013.
[7] M. D. Ulriksen, D. Bernal, L. Damkilde, Input shaping for steady-state damage localization, To appear (2017).
[8] N. C. Singer, W. P. Seering, Preshaping command inputs to reduce system vibration, Journal of Dynamic Systems, Measurement, and Control 112 (1988) 76–82.
[9] K. Hasselmann, Measurements of Wind-wave Growth and Swell Decay During the Joint North Sea Wave Project (JONSWAP), Deutsche Hydrographische Zeitschrift, Deutsches Hydrographisches Institut, 1973.
[10] J. R. Morison, M. P. O'brien, J. W. Johnson, S. A. Schaaf, The force exerted by surface waves on piles, AIME Petroleum Transactions 189 (1950) 149–157.
[11] M. E. Nielsen, M. D. Ulriksen, L. Damkilde, Sofia - a simulation tool for bottom founded and floating offshore structures, in: Proc. X International Conference on Structural Dynamics, EURODYN 2017, 2017.